Computation and Design of Moving Boundary Systems

Wei Shyy
Hong Kong University of Science and Technology
weishyy@ust.hk
Dr. C.-K. Kang, Dr. C.-K. Kuan
University of Michigan

Multiphase Flows - Topologically Varying Moving Boundaries

Multiphase flow in Engineering problems

- ❑Cryogenic liquid in rocket fuel tanks
- ❑Droplet collision/atomization in combustor
- ❑Micro-fluidic devices

Challenges of interfacial flow computation

- ❑Multiscale behavior
- ❑Surface tension/phase change modeling
- ❑Discontinuous fluid properties
- ❑Interface break-up/merge
- ❑Complex solid geometries

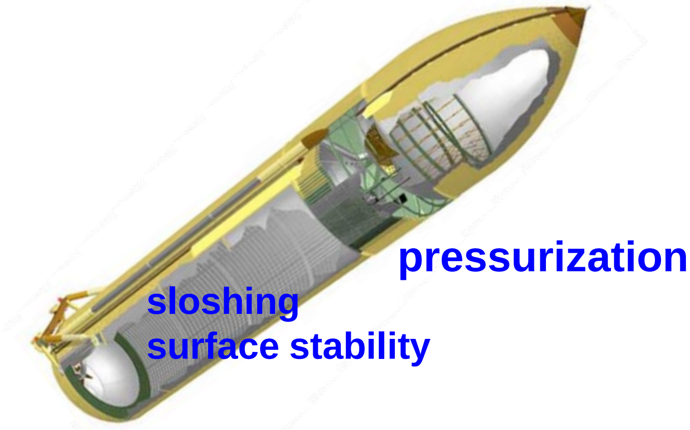

GE Genx Engine B747-7, B787

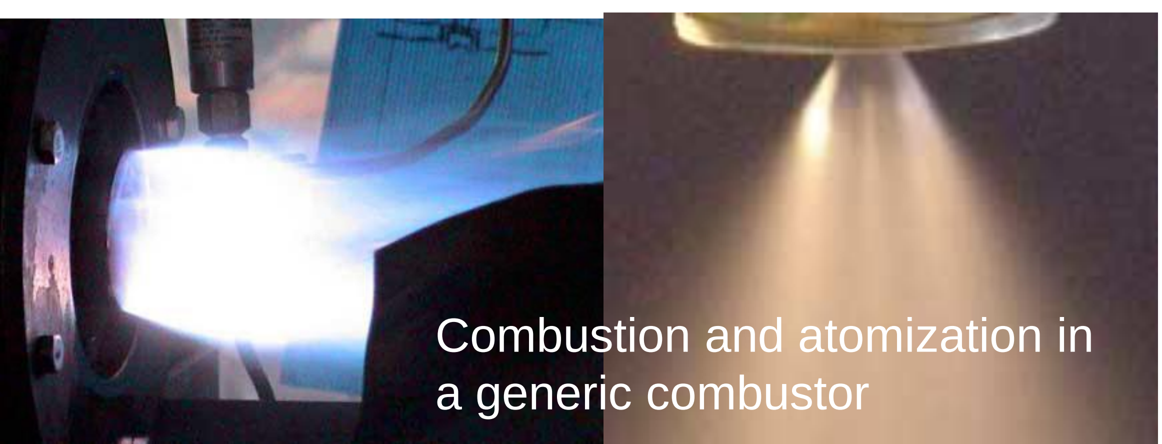

Atomization Dynamics

Global dimensionless parameters

- **Weber number** $We = \dfrac{\rho_l U_0 D_0}{\sigma}$
  - Inertia vs. surface tension vs. viscosity
  - **Free surface flow at varying We, including topological changes due to break-up/merger**
    - small Weber number: maintaining spherical shape
    - large Weber number: unstable → break up as ligaments and droplets
  - Injector Weber number in combustor chamber – $O(10^5)$ or higher
    - unstable impingement sheet→ fragment to ligament
    - Secondary droplet-droplet collision at $We_d \sim O(1)$ to $O(10^3)$

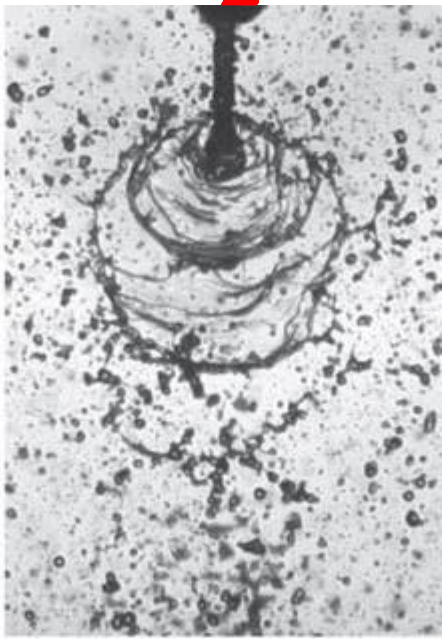

- **Reynolds number** $\mathrm{Re} = \dfrac{\rho D_0 U_0}{\mu_l}$

- **Ohnesorge number** $Oh = \dfrac{\mu_l}{(\sigma \rho D_0)^{1/2}}$

Direct simulation very challenging even without turbulence

Atomization versus Weber Number

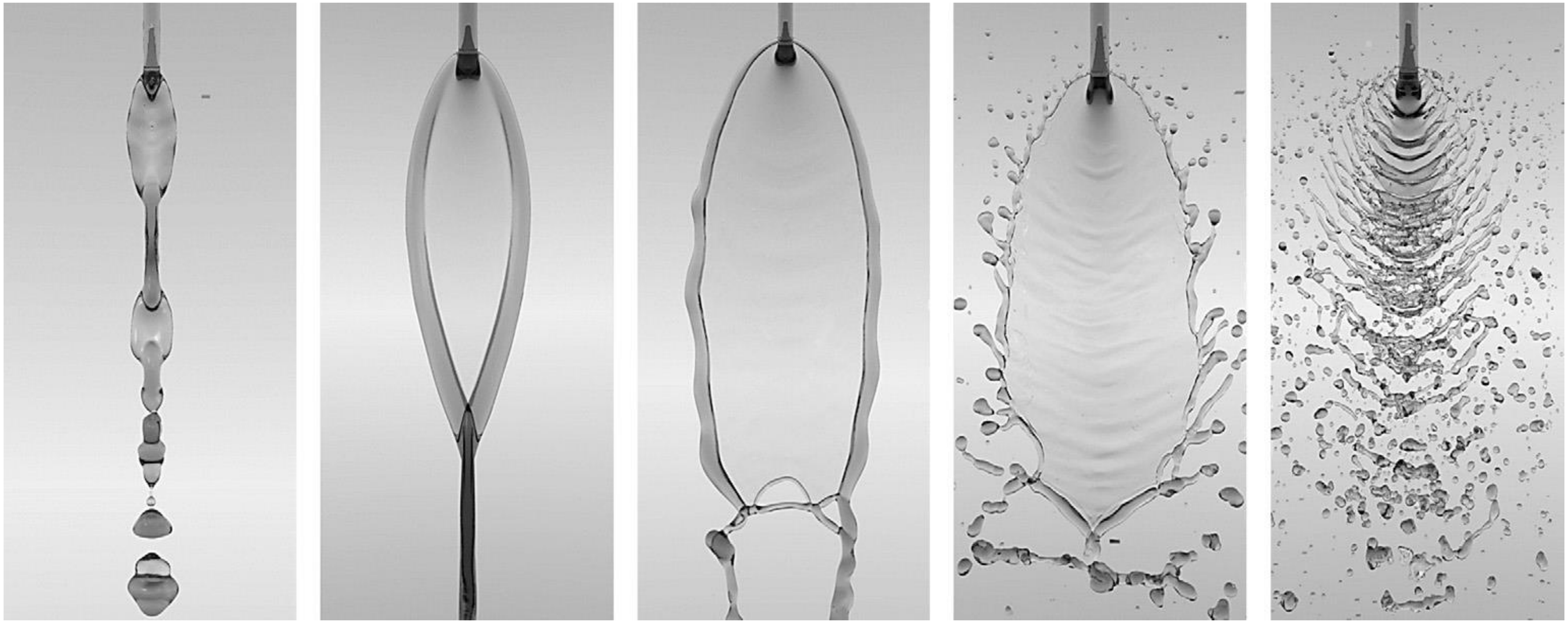

Low ---→ High

Chen & Yang '14 JCP

- High Weber number regime critical to propulsion and power devices
- Challenging to measure/compute due to time/length scale disparity
- Little information on detailed droplet collision dynamics

Combined Eulerian-Lagrangian Method with Local Adaptive Mesh Refinement

Cut-plane view of dynamic adaptive mesh and interface profile

Cell-based unstructured adaptive mesh refinement

- Highly flexible cell-by-cell adaptation

- Unstructured data:
  - Performance of field equations solver is independent of refinement level.
    - No tree-like hierarchy (constant data-fetching cost)
    - No level-level interpolation (communication)

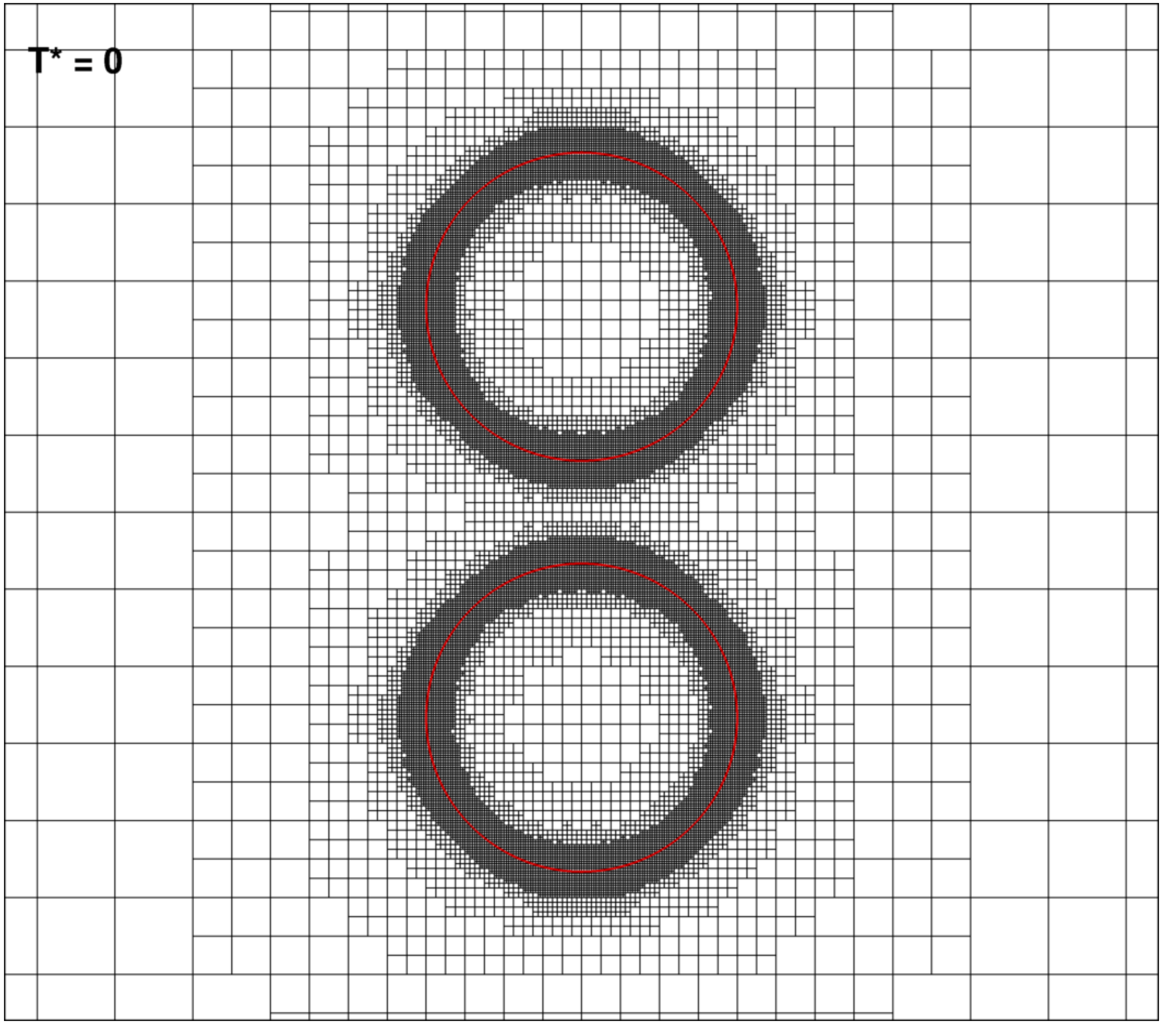

Low Weber Number regime

Computational Parameters

Density ratio = 666.1; Viscosity ratio = 179.3

$$Re = \frac{\rho_{drop} U_{impact} d}{\mu_{drop}}$$

$$We = \frac{\rho_{drop} U_{impact}^2 d}{\sigma}$$

Impact Parameter, $B = h / d$

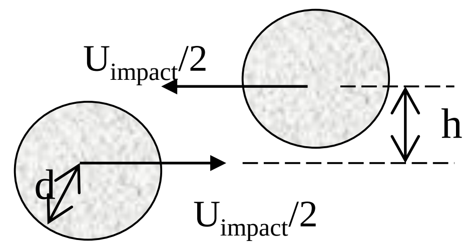

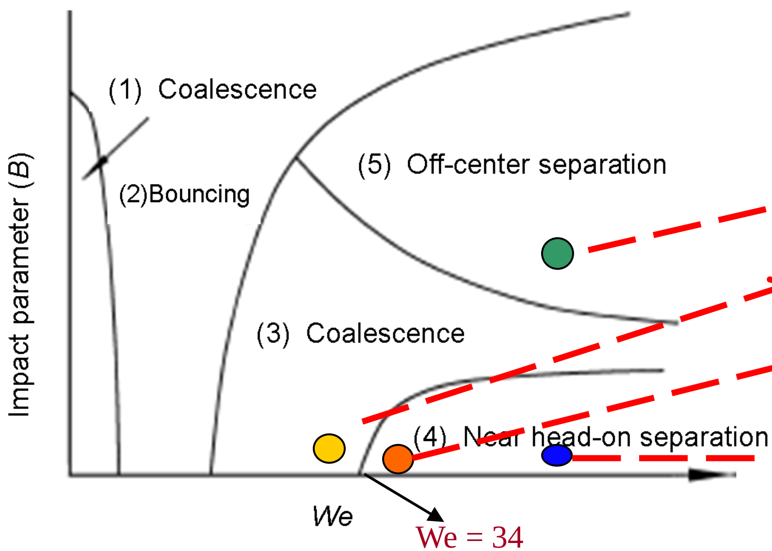

Schematic of collision regime

Case	We	B	Re	Outcome (Qian & Law, 97)
1	60.1	0.55	302.8	Separation with satellite
2	32.8	0.08	210.8	Coalescence
3	37.2	0.01	228.0	Separation
4	61.4	0.06	296.5	Separation with satellite

CASE (1): Off-Center Separation (We = 60.1, B = 0.55) higher Weber # & impact factor

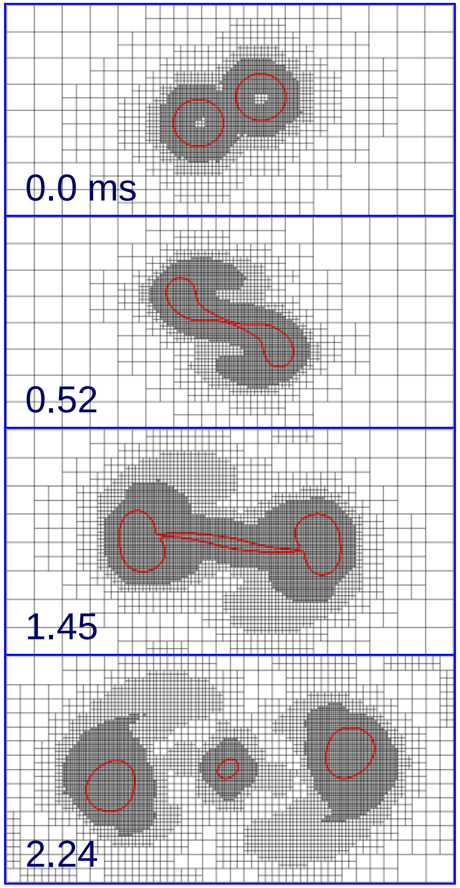

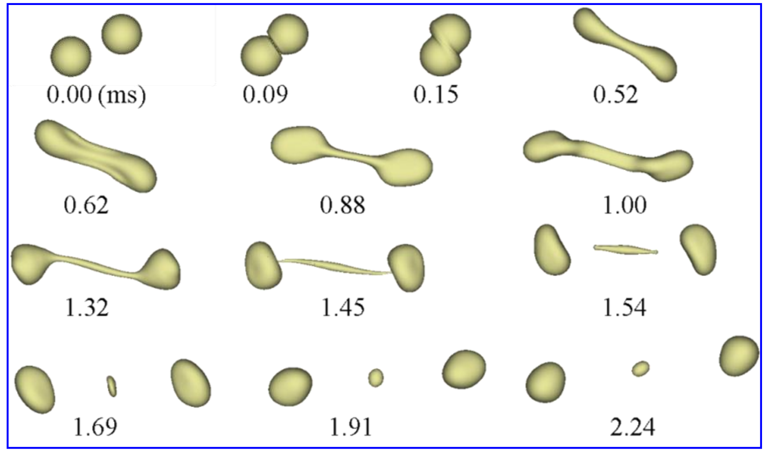

Present computations

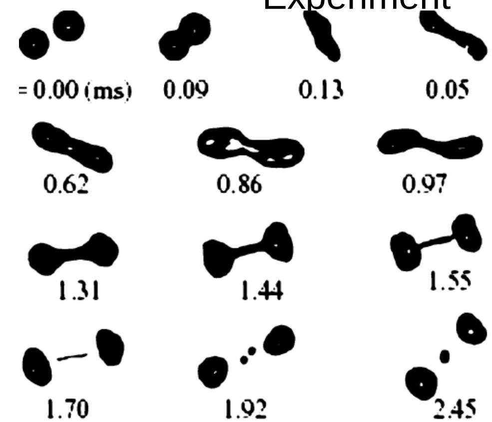

Qian & Law JFM 1997

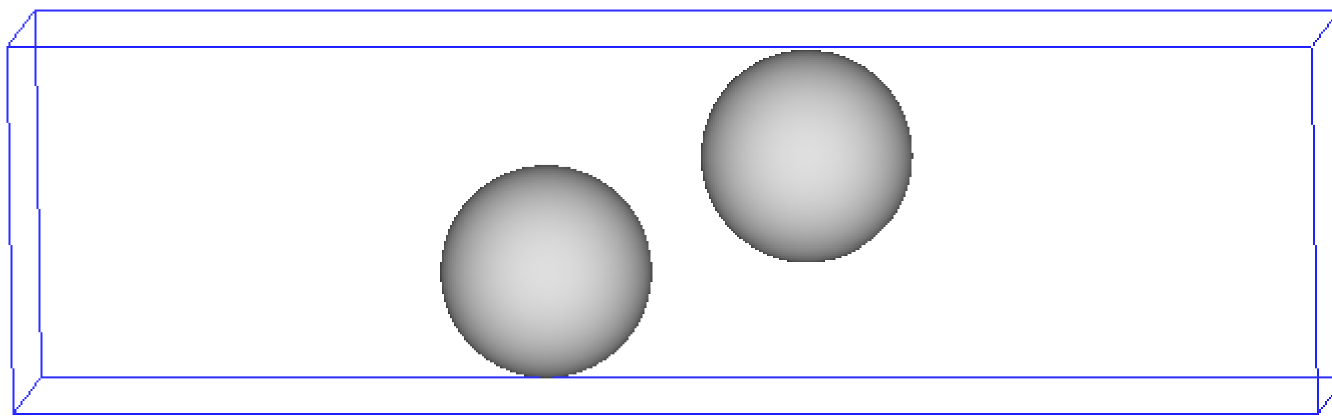

Singh & Shyy, JCP 2007
Kuan, Pan & Shyy, JFM 2014

Binary droplet collision at high Weber number

Motivation

- To improve the understanding of morphologies and instabilities of free surface
- Collisions at the low Weber number regimes were explored by experiments [1] and numerical computations.
- Analysis at high Weber number regimes (from 200 to thousands) is much challenging
  - Experiment at Weber number 200-5000 (Pan et al.[2])
    - Fingering, fingering and separation, breakup, prompt splattering
  - Instabilities
  - Gas-liquid interfaces appear in multiple length scale → costly computation

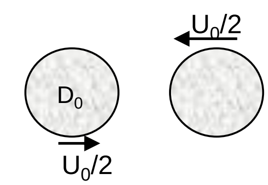

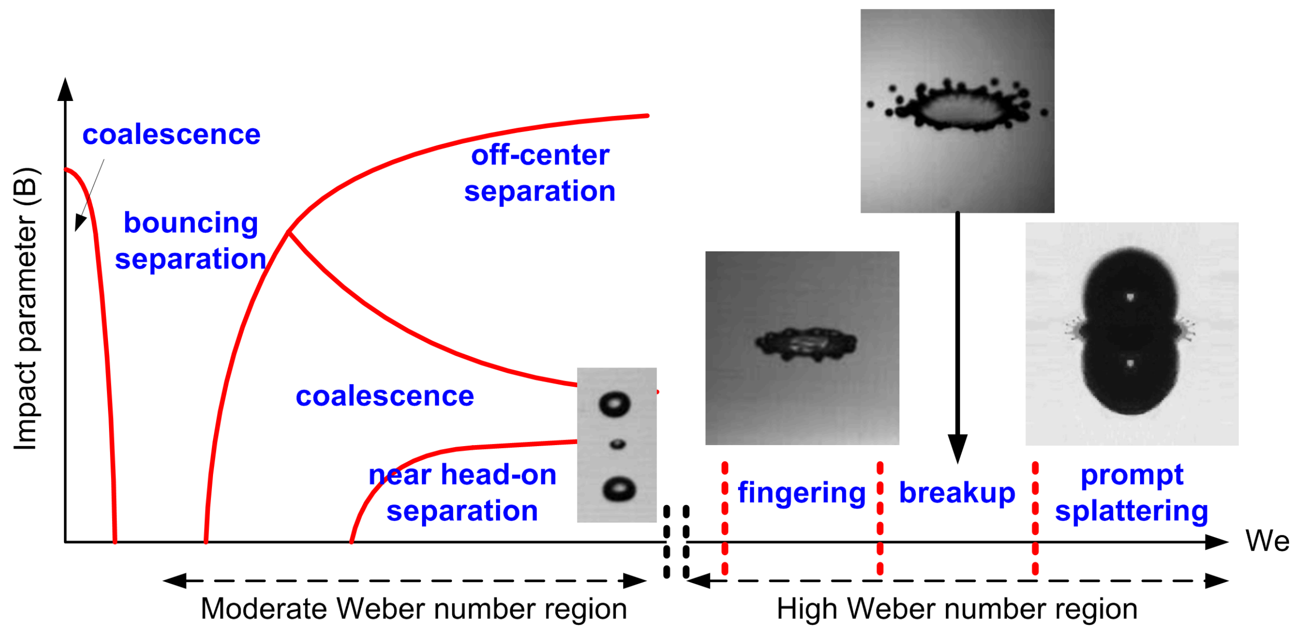

Pan, Chou & Tseng, Physical Review E, 80, 2009
Kuan, Pan & Shyy, J Fluid Mech, 2014.

Droplet collision at high Weber number - validation

We 210

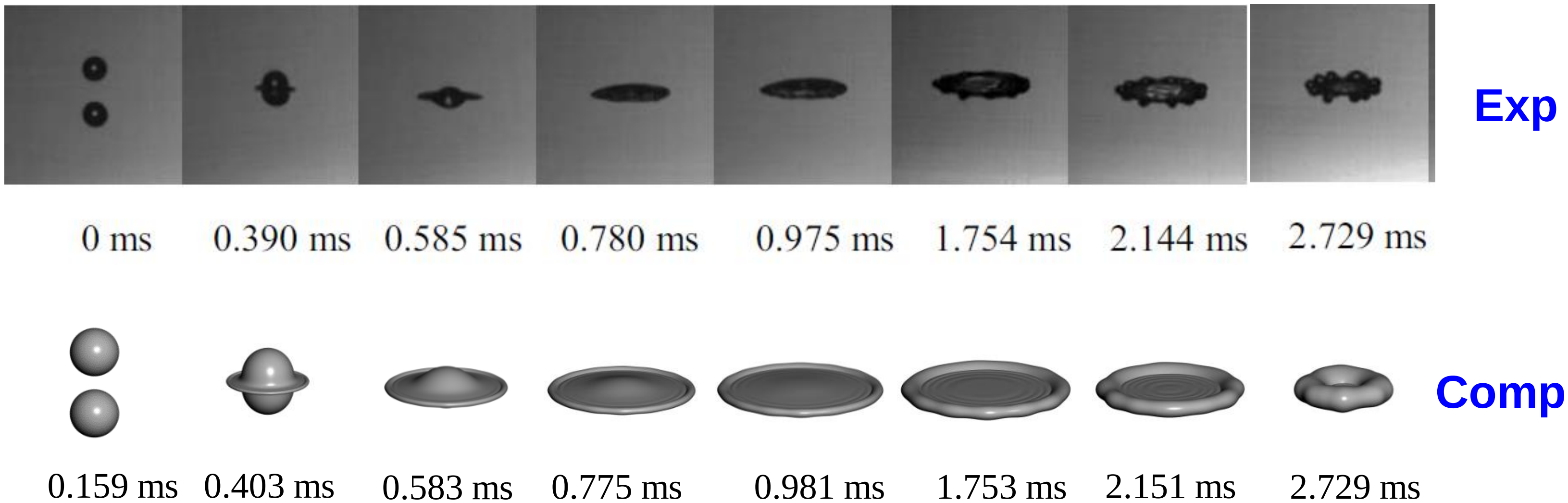

We 277

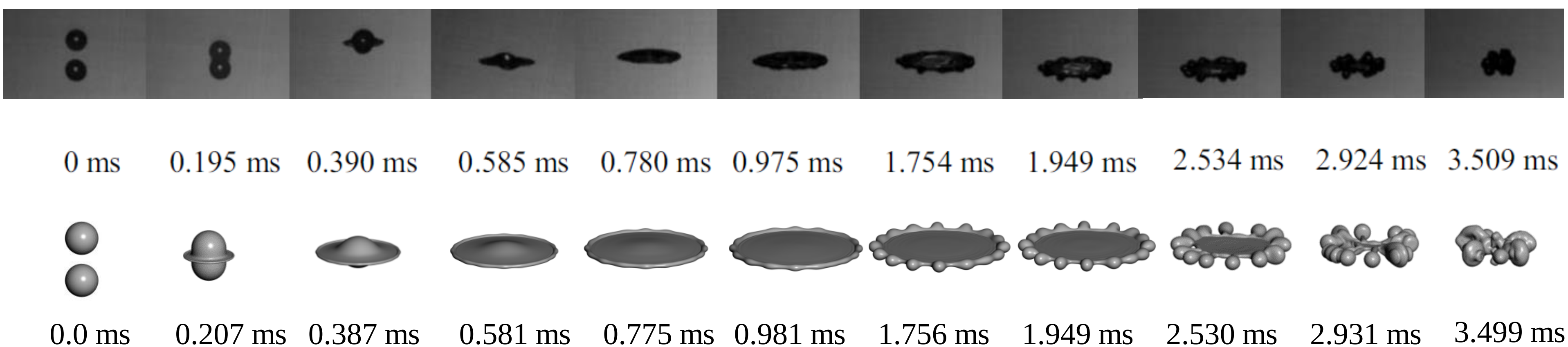

Droplet collision at high Weber number - validation

We 442

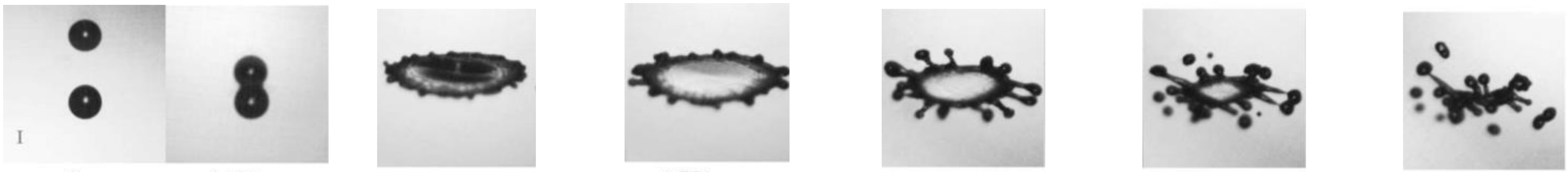

0 ms | 0.195 ms | 1.170 ms | 1.754 ms | 2.729 ms | 3.119 ms | 3.509 ms

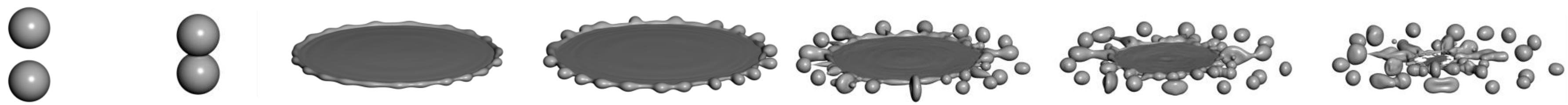

0.101 ms | 0.195 ms | 1.174 ms | 1.752 ms | 2.730 ms | 3.120 ms | 3.509 ms

We 878

0 ms | 0.195 ms | 0.390 ms | 0.585 ms | 0.780 ms

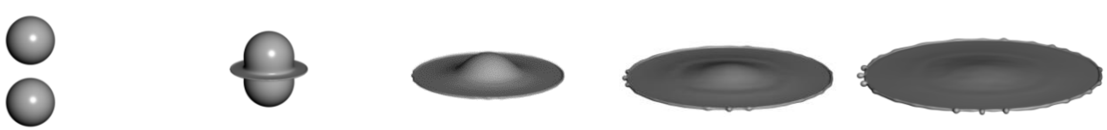

0 ms | 0.195 ms | 0.390 ms | 0.585 ms | 0.780 ms

We 1520

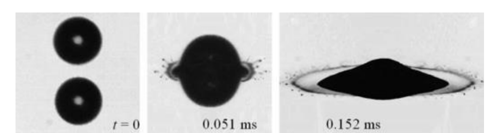

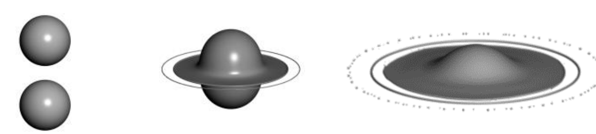

0.000 ms | 0.053 ms | 0.091 ms

Interface evolution: General observation

The merged droplet extrudes a circular sheet

A toroid rim attached to the sheet

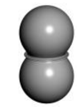

Longitudinal instability on the rim

Rim Inertia >> surface tension force

No

Rim grows with bead-like structures

The rim retract or slowdown

fast

The rim retracts and aggregate

mild

Fingering at retracting phase; disintegration

slowdown

Fingering/necking and then disintegration of the rim

Yes

The rim separates from the disk and continues to expand in radial direction

Necking and thinning of the detached rim →breakup

We 210 and 270

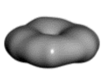

We 442

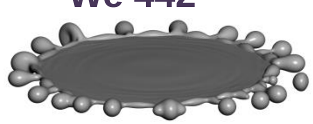

We 688 and 878

We 1120 and 1520

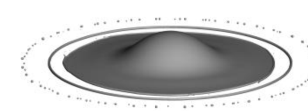

Increasing Weber number →

Droplet collision at high Weber number - animation

- We = 1520 (Eulerian grid size 23 million, Lagrangian marker size 2.5 million)

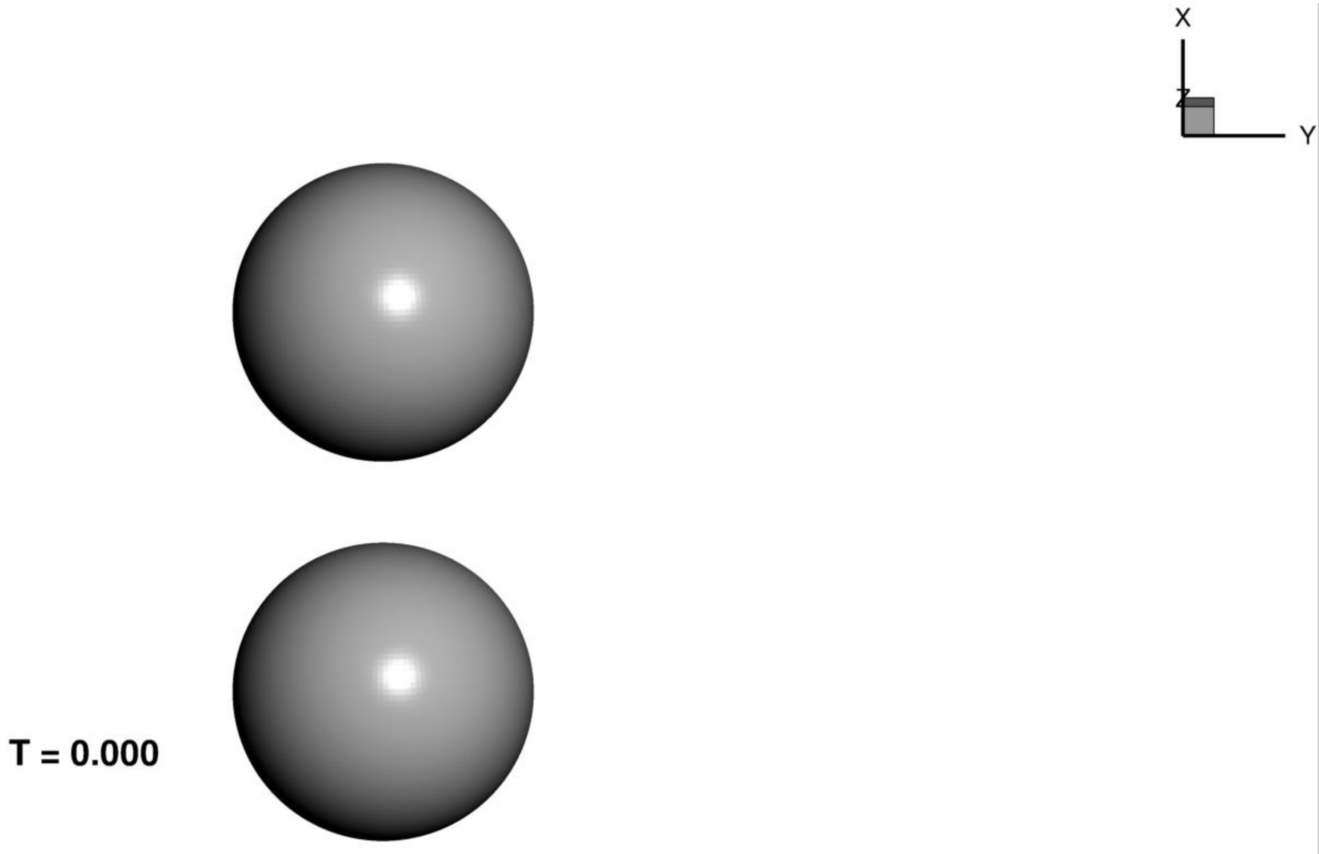

Drop Collision Dynamics Needs to be Incorporated into Atomization Model

Drones in the Sky (WSJ Nov 11, '14)

Google, DJI

DJI and Drone

The New York Times

STATE OF THE ART

Civilian Photography, Now Rising to New Level

Review: The Phantom 2 Vision Photo Drone From DJI

Kit Eaton

What you need to take photos aloft: the Phantom 2 Vision drone, its remote controller and your iOS or Android device.

By KIT EATON
Published: January 1, 2014

FACEBOOK
TWITTER
GOOGLE+
SAVE

Five years ago, the DJI Phantom 2 Vision would have seemed like a science fiction film prop or a piece of surveillance hardware flown only by the sexiest of superspies. But it is the first camera-carrying drone you may want to own — and you could do that without spending thousands of dollars.

TIME

January 30, 2014

REVIEWS

Finally, a Drone You Can Own

The DJI Phantom 2 Vision is a 2.5 pound flying camera

By Alex Fitzpatrick

Remote-controlled aircraft hobbyists have been trying to MacGyver small digital cameras to their airborne contraptions for years. Chinese manufacturer DJI has finally come along and rendered all that tinkering unnecessary, selling what's essentially a flying camera ready-to-go out of the box: The DJI Phantom 2 Vision.

Setup

There's an acronym in remote-controlled flying: "RTF," or "Ready-to-Fly." Many times, products advertise themselves as "RTF" when that's really only half-true—but that's not the case here. All you've got to do to get airborne with the Phantom 2 Vision is charge up the flight battery and Wi-Fi range extender, screw on its four propellers and pop four AA-size batteries into the controller. After you download and set up the mobile app and attach the range extender and phone clip to the controller, you're clear for liftoff.

Flying

I've never met a remote-controlled aircraft quite this easy to fly. At two-and-a-half pounds, it has a heft that's helpful for stability (though I wouldn't risk it on a particularly windy day). The quadcopter's four engines and propellers allow it to maneuver like a helicopter, making it pretty nimble once you get the hang of it—it flies on three axes and can hover with minimal pilot input thanks to its internal GPS system.

The Phantom's control scheme was a little counter-intuitive at first—it would be nice if it was customizable, as is the case with more complex (and often very expensive) RC airplane transmitters. But with a little practice, flying the Phantom gets simple quick. Bringing it back to terra firma manually, however, can be a bit tricky—I damaged a propeller on what might be called a "hard landing." But there's a GPS-based auto-land feature that's useful for the uninitiated, and attaching a new prop was less than a five-minute job with a tool DJI provides for the task. And there's a saying in aviation: Any landing where you can use the plane again is a great landing.

I should probably note that somebody with less R/C flying experience might find the learning curve a bit more steep. Helpful tip: Try to keep the back of the aircraft facing you until you start learning how to "mirror" the controls when it's facing a different direction than you are. It would be neat if DJI provided some kind of game inside its mobile app to get a feel for the controls in a virtual environment before advancing to the real deal.

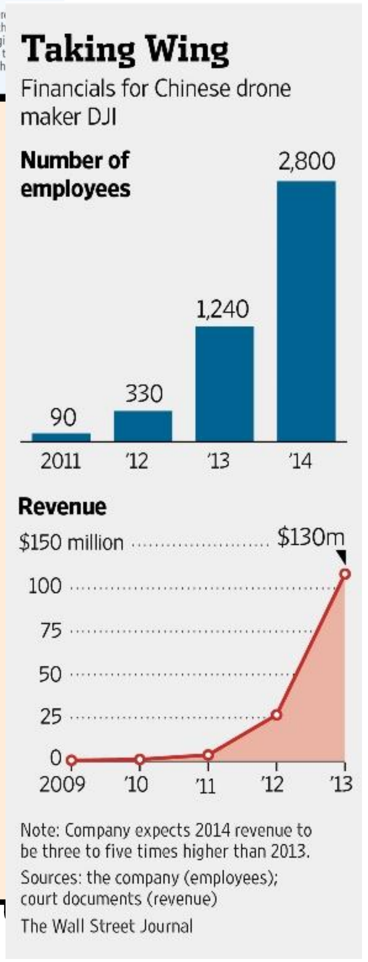

Size vs Flexibility

As vehicle becomes smaller/slower, Re is reduced, wing movement more important, & fluid-structure interaction is more pronounced

Flapping, Flexible Wing

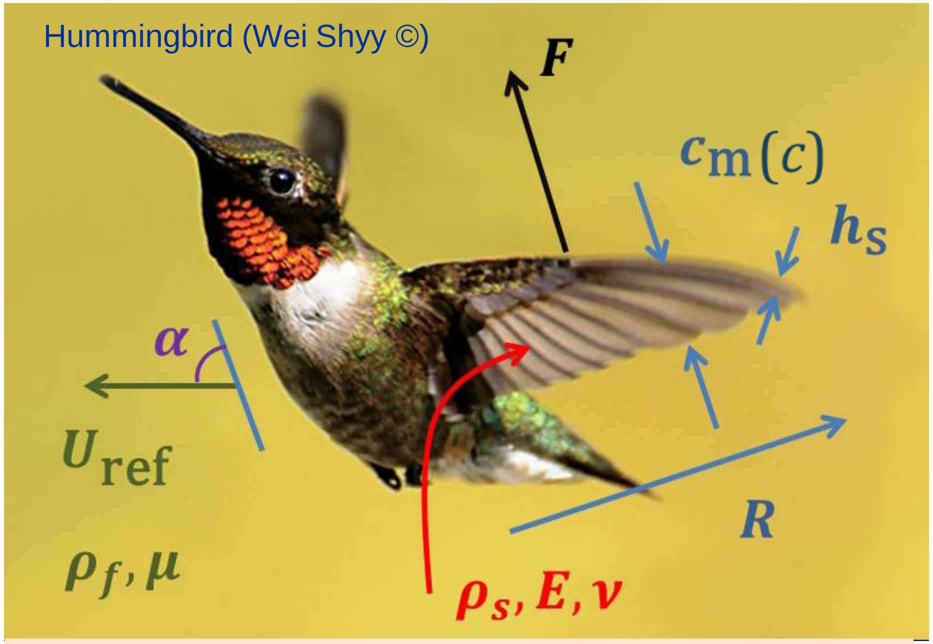

Reynolds number

$$Re = \frac{\rho_f U_{\text{ref}} c}{\mu}$$

Reduced frequency

$$k = \frac{\pi f c}{U_{\text{ref}}}$$

Thickness ratio

$$h_s^* = h_s / c$$

Density ratio

$$\rho^* = \rho_s / \rho_f$$

Frequency ratio

$$f / f_1$$

Effective stiffness

$$\Pi_1 \sim \frac{E h_s^{*3}}{\rho_f U_{\text{ref}}^2}$$

- Velocity scale U_{ref}: max translational velocity
- Strouhal number is a constant in hover
- f/f_1 and Π_1 not independent to each other

$$\Pi_1 \sim \left(\frac{k}{f/f_1}\right)^2$$

Re:	fluid inertia vs. viscosity
k:	unsteadiness
h_s^*:	wing thickness vs. chord
ρ^*:	wing density vs. fluid density
f/f_1:	motion vs. natural frequency
Π_1:	wing stiffness vs. dynamic pressure

Wing Deformation, Lift Generation = $\Psi(Re, h_s^*, \rho^*, k, f/f_1)$

Shyy et al., Intro Flapping Wing Aerodynamics, 2013

Unsteady Lift Mechanisms of Flapping Airfoil

vorticity

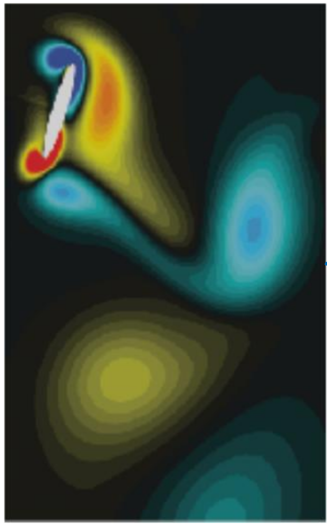

Wake Capture Enhances lift

vorticity

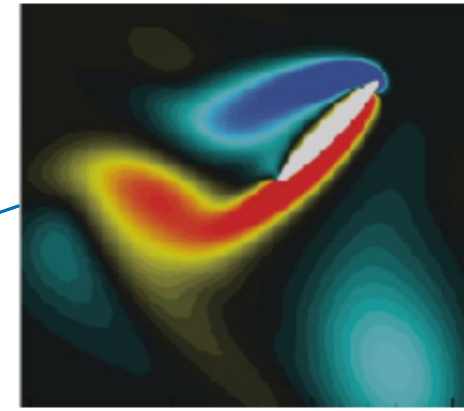

Delayed Stall Enhances lift

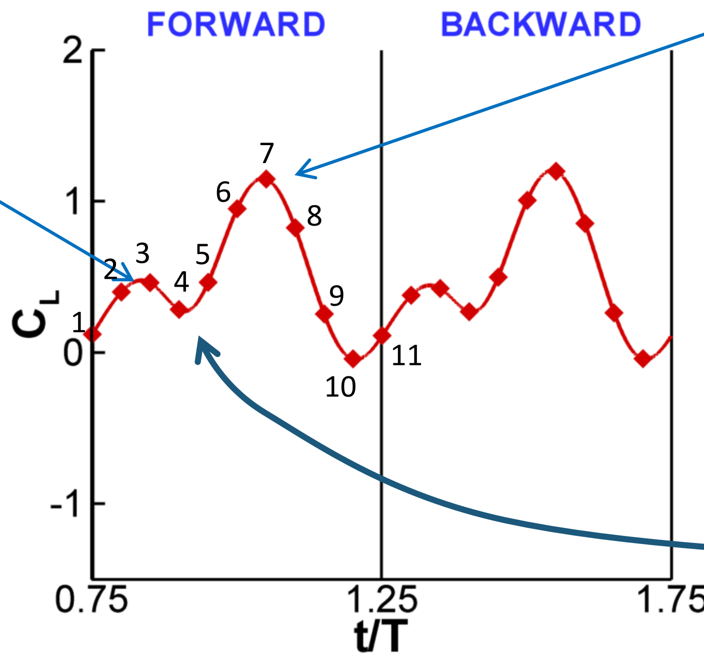

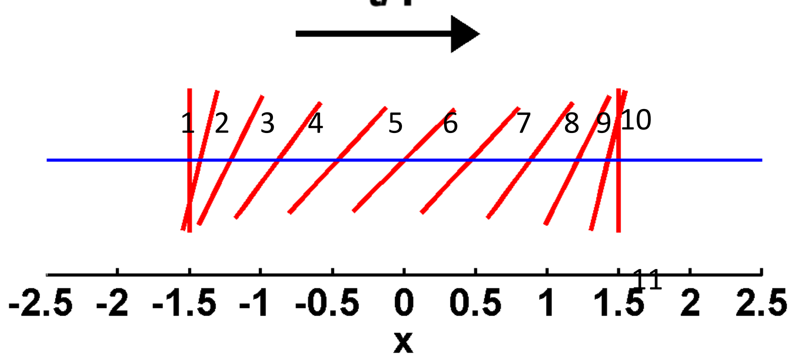

v-velocity

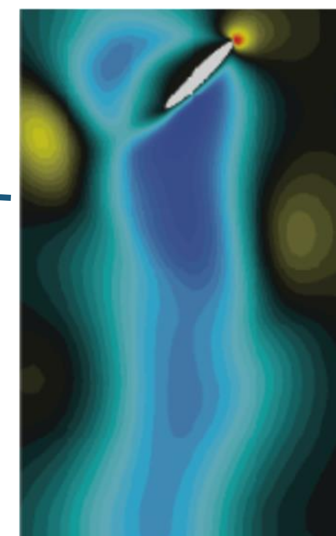

Jet Interaction Reduces lift

Re = 100
$2h_a / c = 3.0$
$\alpha_a = 45°$
$\varphi = 90°$

Unsteady Lift Mechanisms of Flapping Wing

Rotating Starting Vortex Enhances/reduce lift?

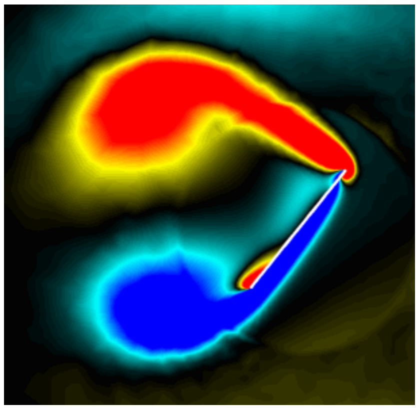

z-vorticity

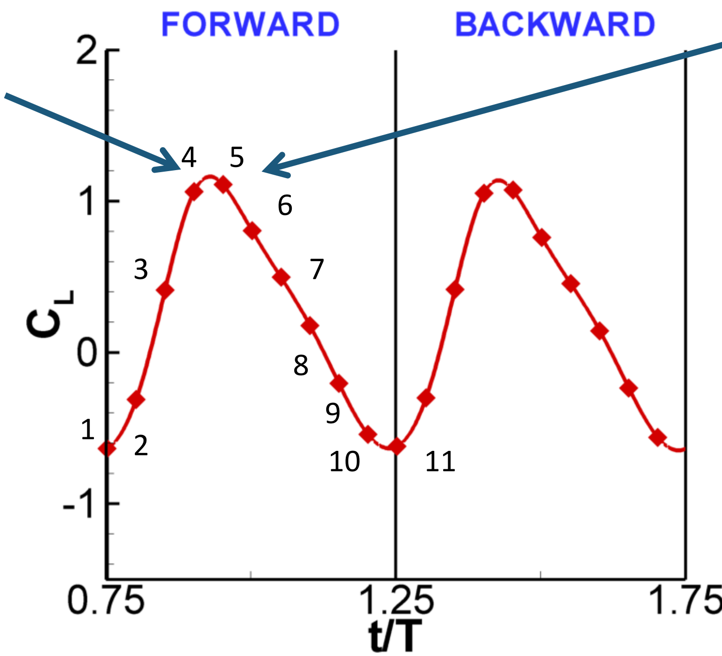

x-vorticity

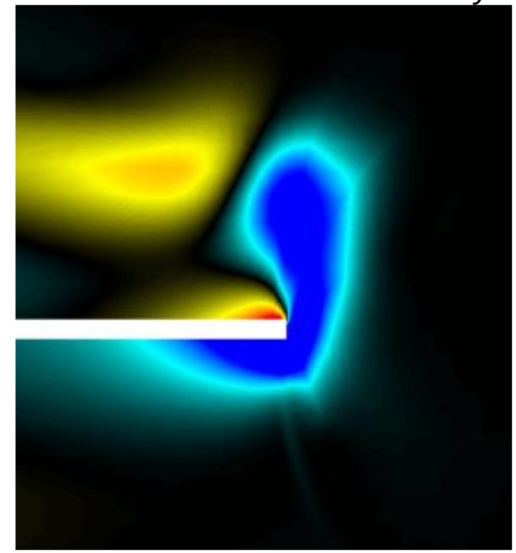

Tip Vortex reduces lift?

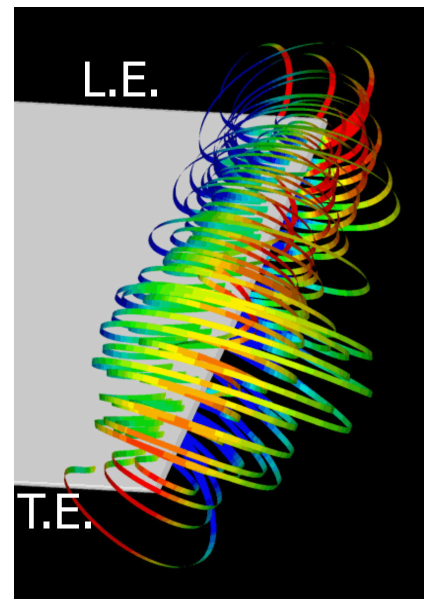

vertical velocity contours on streamlines

Re = 100
$2h_a/c = 2.0$
$\alpha_a = 45°$
$\varphi = 60°$

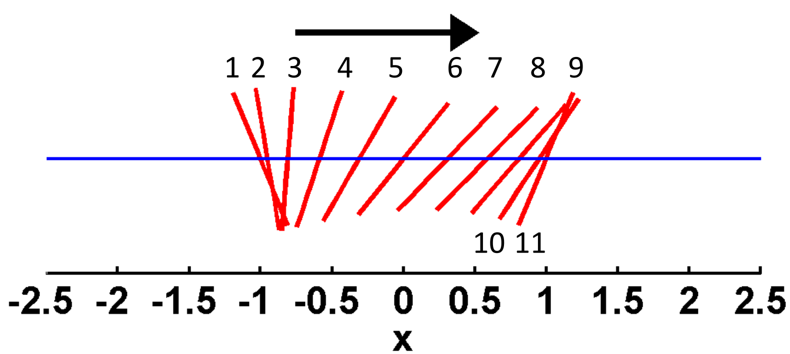

Pareto Fronts: Lift vs. Power of Rigid Wing

Surrogate Model facilitates the investigation

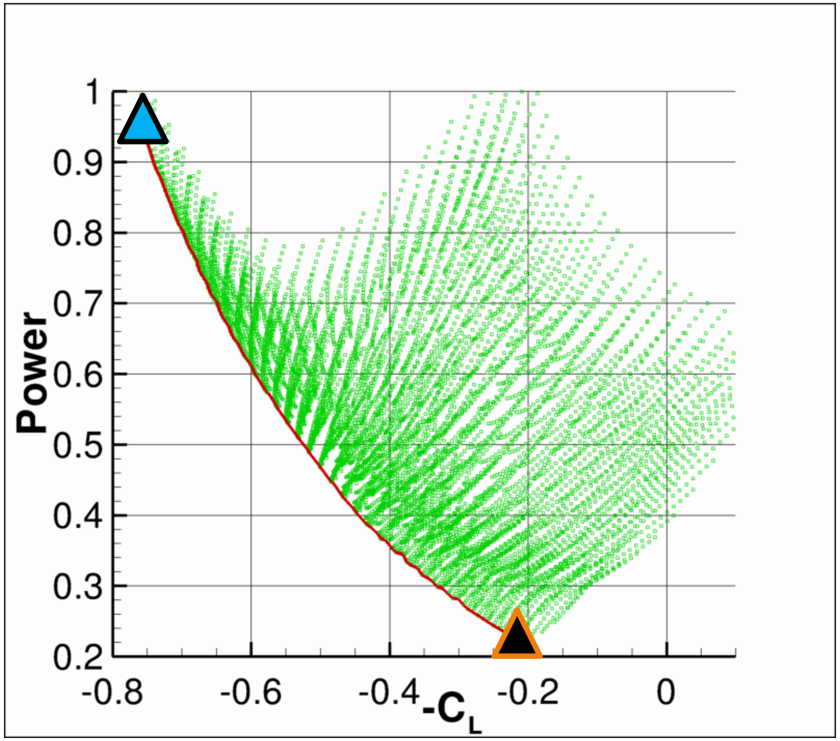

High Lift: Advanced rotation; High AoA

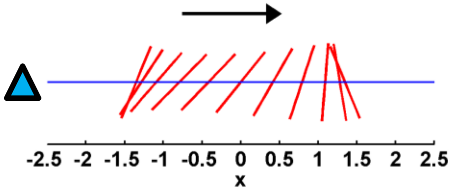

Low Power: Delayed rotation; Low AoA

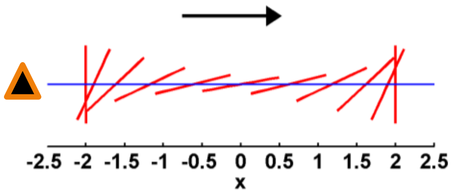

Optimal Lift for Flexible Wing - Symmetric Rotation

Just as for the rigid wings, all three rotational modes are observed:

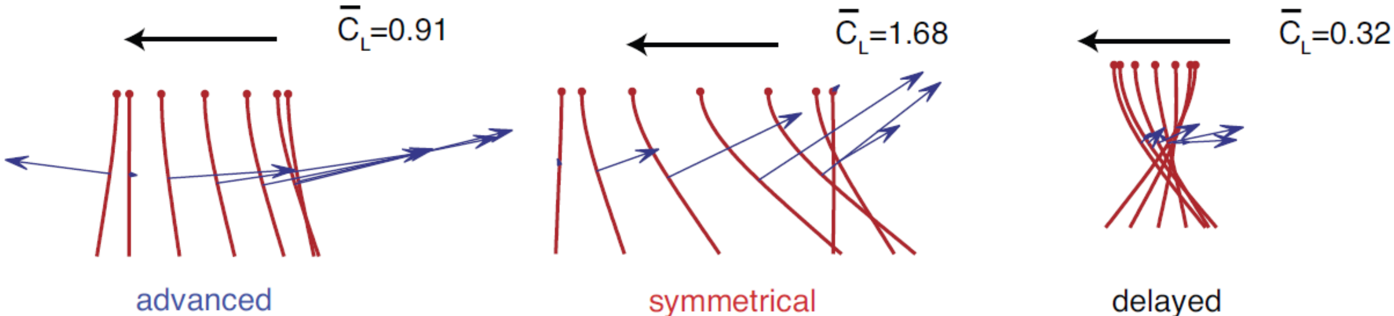

k = 0.95; f/f_1 = 0.15 k = 0.6; f/f_1 = 0.25 k = 2.0; f/f_1 = 0.82

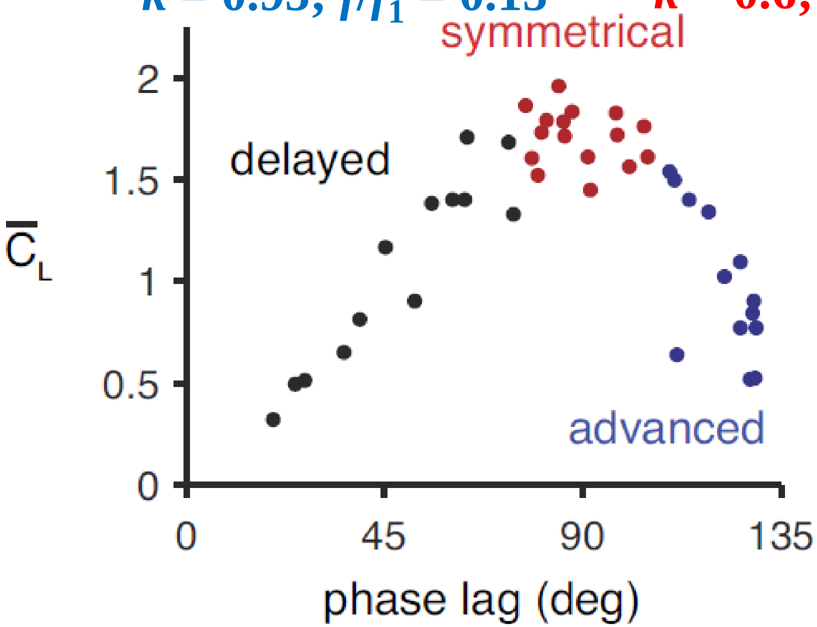

For rigid wings with active rotation, highest lift obtained when:

- slightly advanced rotation
- midstroke angle of 45 – 50 deg

For the flexible wing, the symmetric rotational mode → highest lift (> 1.6) [1]

Kang & Shyy, J Royal Society Interface 2014;
Shyy et al, Intro Flapping Wing Aerodynamics, Cambridge Univ Press 2013

Fluid-Structural Interactions

Fluid

mass: $$\nabla \cdot \boldsymbol{u}^* = 0$$

momentum: $$\frac{k}{\pi}\frac{\partial \boldsymbol{u}^*}{\partial t^*} + \boldsymbol{u}^* \cdot \nabla \boldsymbol{u}^* = -\nabla p^* + \frac{1}{Re}\nabla^{*2}\boldsymbol{u}^*$$

Structure

Π_0 : Effective inertia

$$\overbrace{\boxed{\rho^* h_s^* \left(\frac{k}{\pi}\right)^2 \frac{\partial^2 w_3^*}{\partial t^{*2}}}}^{\Pi_0} + \boxed{\Pi_1 \nabla^{*4} w_3^*} = \boxed{f^*}$$

inertia elasticity aerodynamic force

Π_1: Effective stiffness

$$\Pi_1 = \frac{E h_s^{*3}}{12 \rho_f U_{\mathrm{ref}}^2}$$

Beam: 1D

$$\Pi_1 = \frac{E h_s^{*3}}{12(1-\nu^2)\rho_f U_{\mathrm{ref}}^2}$$

Plate: 2D

Kinematics

$$h^* = St\frac{\pi}{k}\cos(2\pi t^*)$$

Non-dim. variables

$$(\quad)^*$$

Reynolds number

$$Re = \frac{\rho_f U_{\mathrm{ref}} c_m}{\mu}$$

Reduced frequency

$$k = \frac{\omega c_m}{2U_{\mathrm{ref}}}$$

Density ratio

$$\rho^* = \rho_s/\rho_f$$

Thickness ratio

$$h_s^* = h_s/c_m$$

Strouhal number

$$St = \frac{k}{\pi}\frac{h_a}{c_m}$$

Non-dimensionalized with Velocity: U_{ref} Length: c_m Time: $2\pi/\omega$

Force Deforming a Flexible Wing

vortex impulse

$$C_F \sim \frac{h_a}{c}\left\{\frac{1}{Re}O(1) + St\,O(1)\right\} + St\,k\,O(1)$$

viscous $\sim f^0$ inertia $\sim f^1$ added mass $\sim f^2$

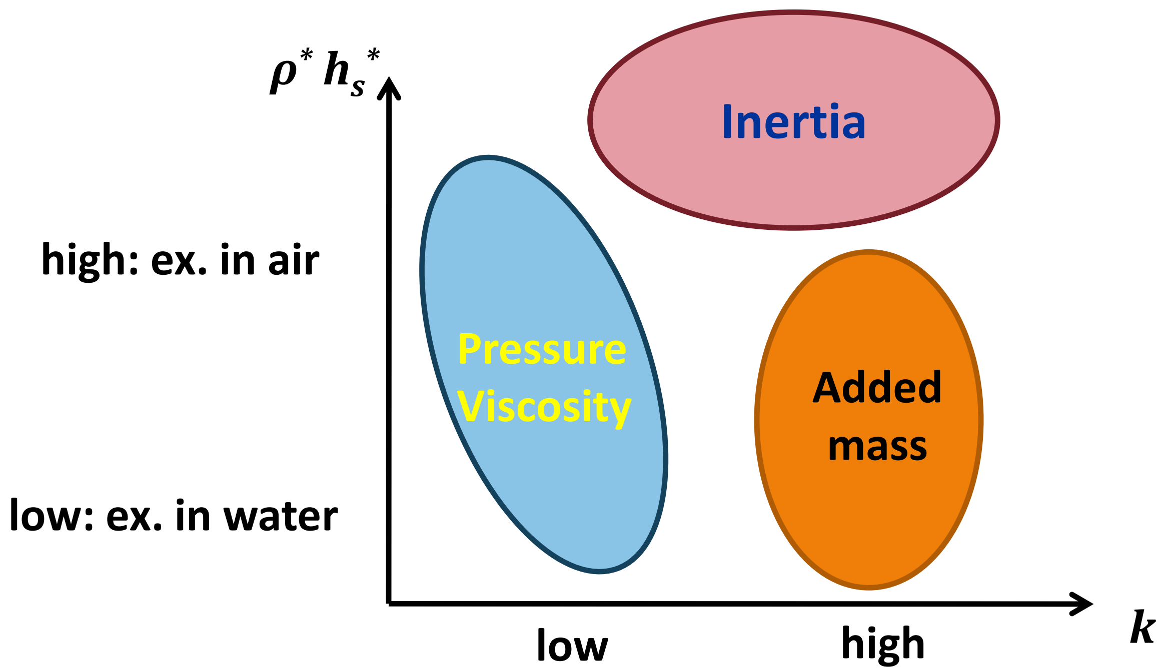

- Global assessment for preliminary design: scaling parameters
- Stress distribution for aerodynamics/control design: Kinematics, shape, properties

Scaling for

Force Generation

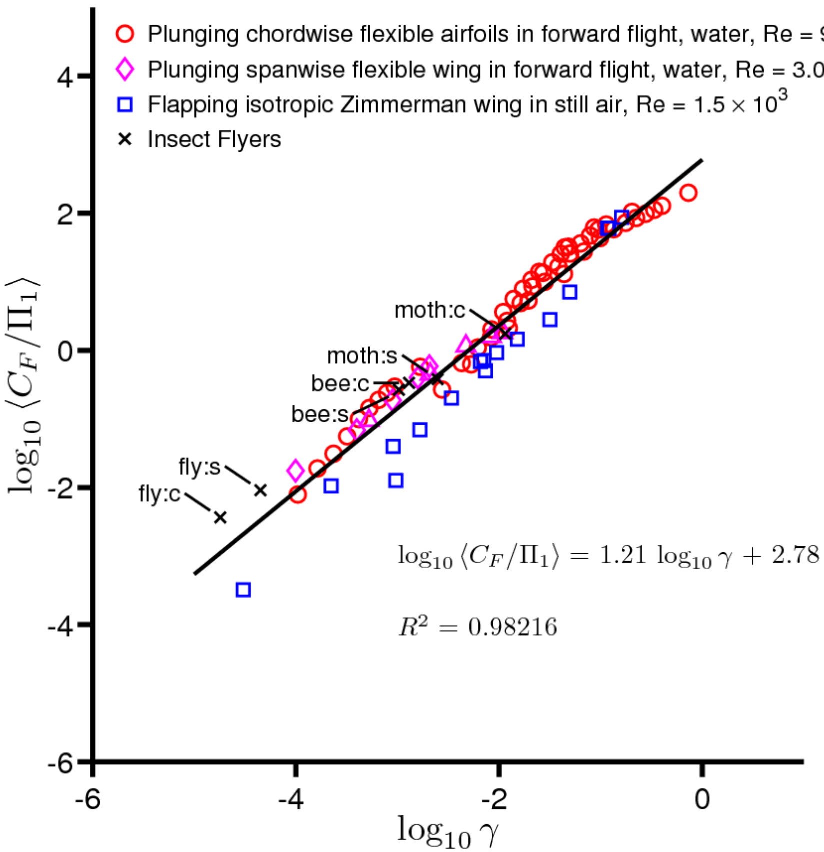

$$\boxed{\frac{\langle C_F \rangle}{\Pi_1} \sim \gamma}$$

Power Input

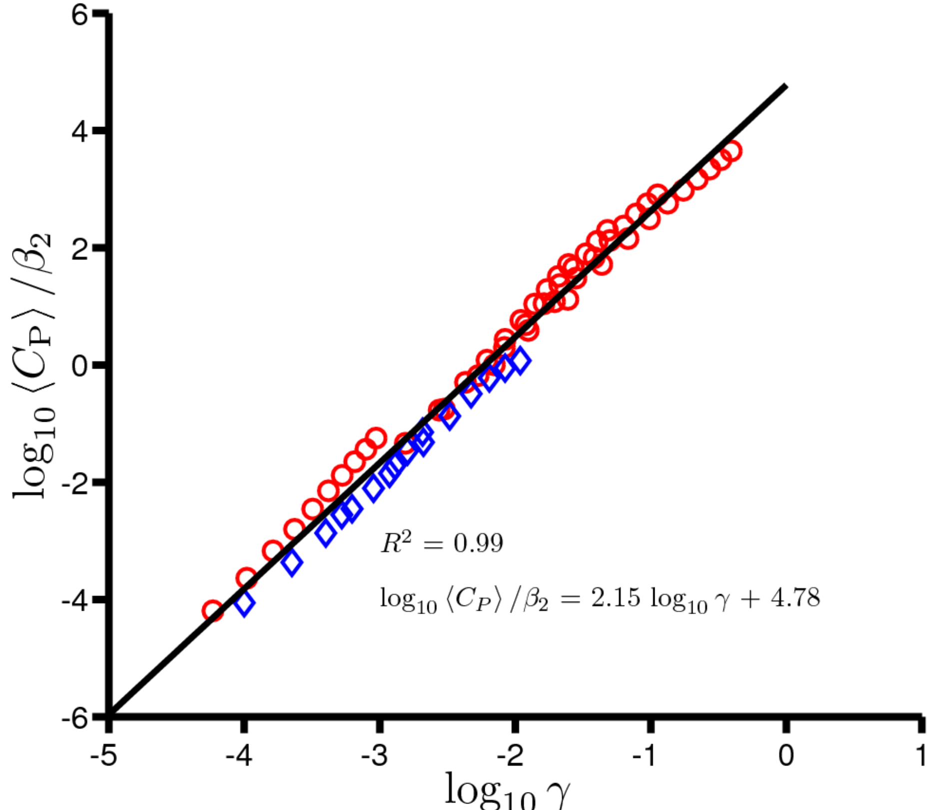

$$\frac{\langle C_P \rangle}{\beta_2} \sim \gamma^2 \qquad \beta_2 = \frac{\Pi_1^2}{k^2 + 4\pi\Pi_0}$$

mean force / effective stiffness ~ max. relative wing tip deformation

Frequency Selection Optimal Propulsive Efficiency

$$\boxed{\eta = \frac{\langle C_T \rangle}{\langle C_P \rangle}}$$

Propulsive efficiency scaling

$$\eta \sim \left\{1 - \left(\frac{\omega}{\omega_1}\right)^2\right\}^{0.82} \omega^{0.36}$$

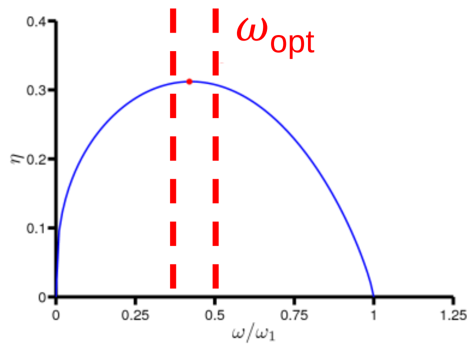

Current study

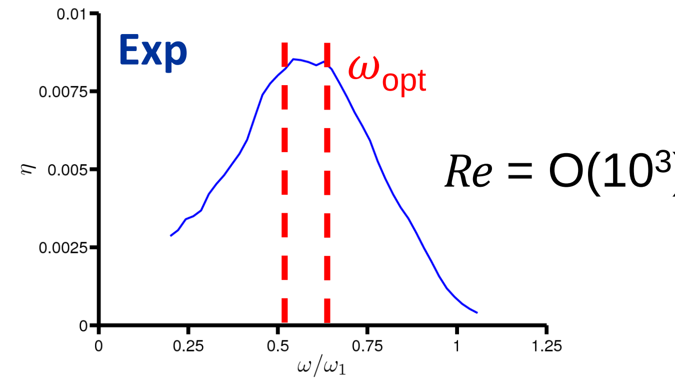

Ramananarivo et al. (2011)

Literature	ω_{opt}	Description
Vallena et al. (2009)	0.3	Hover, 2D airfoil, torsion spring model
Yin & Luo (2010)	0.4-0.5	Hover, 2D airfoil, membrane model
Ramananarivo et al. (2011)	0.5-0.6	Self-propelled flapper experiment
Current study	**0.4-0.5**	**Scaling analysis**

Example 1: 2% thick aluminum wing with 20 cm chord, 50 cm half span

→ motion frequency: 6.6 Hz for optimal propulsion

Example 2: 2% thick aluminum wing with 2 cm chord, 5 cm half span

→ motion frequency: 55 Hz for optimal propulsion